Sr impurity effects on the magnetic correlations of $La_{2-x}Sr_xCuO_4$

R. J. Gooding and N. M. Salem
Department of Physics, Queen's University, Kingston, Ontario K7L 3N6, Canada

R. J. Birgeneau and F. C. Chou
Department of Physics and the Center for Materials Science and Engineering, Massachusetts Institute of Technology, Cambridge, Massachusetts 02139

(Received 25 September 1996)

We examine the low-temperature magnetic properties of moderately doped $La_{2-x}Sr_xCuO_4$, paying particular attention to the spin-glass phase and the commensurate-incommensurate transition as they are affected by Sr impurity disorder. A model of the carriers, believed to be appropriate at low temperatures, is employed in the CuO_2 planes that accounts for both the strong coupling of the hole's motion to the antiferromagnetically correlated spins and the pinning potential associated with the Sr impurities. This model has been shown to explain quantitatively several magnetic and transport features of the antiferromagnetic region of the phase diagram. Preliminary indications that this model also can explain the $x \geqslant 0.02$ region of the phase diagram follow from its success in accounting for the doping and temperature variation of the spin correlation length. Here we further scrutinize this model by attempting to explain various features of the spin texture of the spin-glass phase. New measurements with traveling-solvent float zone grown crystals of the low-temperature susceptibility show an increase of an anomalously small Curie constant with doping. This behavior is modeled in terms of our numerical simulation results that find small clusters of antiferromagnetically aligned regions separated by disordered domain walls produced by the impurities — the domain walls lead to a percolating sequence of paths connecting the impurities. We predict that for this spin morphology the Curie constant should scale as $1/[2\xi(x,T=0)^2]$, ξ being the spin correlation length, a result that is quantitatively in agreement with experiment. Also, we find that the magnetic correlations in the ground states produced by our simulations are commensurate in the spin-glass phase, consistent with experiment, and that this behavior will persist at higher temperatures where the holes should move along the domain walls effectively being expelled from the antiferromagnetically correlated domains. However, our results show that incommensurate correlations develop continuously around 5% doping with an incommensurate wave vector along $[(\pm 1,0),(0,\pm 1)]$, consistent with recent measurements by Yamada *et al.* At this doping level the domain walls and not the clusters start to become the dominant feature of the spin texture, and thus the Curie behavior should disappear in the incommensurate phase, again consistent with experiment. Thus, we find that this model is capable of describing the low-temperature disorder-induced magnetic spin morphologies of the $La_{2-x}Sr_xCuO_4$ system in the low and intermediate doping regions of the phase diagram. Coupling this understanding of the magnetic correlations with the observed transport features, it is clear that *impurity effects strongly influence the physics of LaSrCuO.* [S0163-1829(97)01210-1]

I. INTRODUCTION

The magnetic, electronic, and transport behavior of the $La_{2-x}Sr_xCuO_4$ high-T_c superconductor have been intensely studied, and one avenue of research that might lead to an understanding of the anomalous normal-state properties, as well as possibly the key to the superconducting instability, involves the examination of the evolution of the antiferromagnetic (AFM) insulator ($0.0 \lesssim x \lesssim 0.02$) to a spin-glass (SG) phase ($0.02 \lesssim x \lesssim 0.05$), and ultimately to a superconductor with anomalous normal-state properties ($0.05 \lesssim x \sim 0.2$). Each of these doping ranges involve new and exciting physics with many mysteries to resolve,[1,2] and in this paper we focus on the microscopic details of the spin texture of the SG phase.

Early experimental work demonstrated that the $0.02 \lesssim x \lesssim 0.05$ materials had a low-temperature SG phase, as evidenced in the freezing of the magnetic moment seen in μSR studies.[3] Shortly afterward it was noted that quasielastic-neutron-scattering results for this phase[4] could be interpreted in terms of the freezing of microdomains roughly of a size of 20 Å. Subsequent NQR experiments supported this conjecture by showing how the La relaxations rates could be understood in terms of AFM domains of small, finite-size magnetic domains.[5] These interpretations made it quite natural to refer to this phase as a cluster SG.

More recent experiments have provided a much more complete characterization of these compounds. Most importantly, the measurements show evidence of canonical SG behavior.[6] Further, samples in this doping range are found to have an anomalously small Curie constant as one approaches the SG transition from above.[6] Also, studies of the anomalous transport properties,[7] including an isotropic, negative magnetoresistance,[8] serve to emphasize the unusual behavior of LaSrCuO in this doping regime at low temperatures.

In this paper we discuss how the spin texture of the SG phase at a microscopic level (i) necessitates the identification of this phase as a cluster SG, and (ii) explains how the small

finite-size domains characterizing this spin texture are consistent with the anomalously small Curie constant found experimentally. To do this, we must begin with a model for the effect of the dopant Sr impurities and the holes they induce into the CuO_2 planes. However, if a model is to be successful in describing the physics of this compound, it must be able to describe the physics in *all* doping ranges, not simply the SG regime. We employ such a candidate model — it was introduced previously[9,10] and is based on the strong coupling of the hole's motion to the background antiferromagnetic Cu-spin correlations. To be specific, at low temperatures, when the carriers are localized in the region of the Sr impurities, they generate spin distortions that one can model using a spin-only Hamiltonian. Our model is only strictly justified at low temperatures where the carriers are localized near the Sr impurities — however, as has been argued elsewhere,[10] and as we elaborate on below, we believe that the spin distortions produced by the holes that gradually become mobile as the temperature is raised will resemble those generated by the localized carriers that we focus on in this paper, and thus the qualitative aspects of the arguments presented here should be applicable at higher temperatures.

This model accounts for the crucial and largely ignored role (in previous literature) of dopant *disorder*. To be specific, when comparing its predictive powers to the physics of the weakly doped AFM phase this model has been shown to be capable of describing (i) the traverse spin-freezing temperature vs doping[11] observed by Chou *et al.*,[12] and (ii) provides a better fit to the conductivity vs T data than three-dimensional (3D) variable-range hopping, as well as correctly predicting the critical concentration $x_c \approx 0.02$ at which the metal non-metal transition takes place.[13,14] Further, when compared to the behavior of the intermediate doping regime for the SG phase, preliminary work[10] showed that this model is able to track the behavior of the doping and temperature-dependent spin correlation length, as measured by Keimer *et al.*[7] and characterized by the empirical relationship

$$\xi^{-1}(x,T) = \xi^{-1}(x,0) + \xi^{-1}(0,T). \tag{1}$$

In this paper we continue the comparison of our candidate model by studying its spin texture vs doping in the SG regime. We focus on understanding the spin texture at a microscopic level and find that disorder induces meandering domain walls connecting Sr sites; we argue that this is the correct way to think of the underlying spin texture of a cluster SG. A state qualitatively similar to this but one produced by electronic phase separation in the presence of Sr impurity disorder was previously proposed by Emery and Kivelson.[15] In our model the possibility of electronic phase separation does not exist, and so electronic phase separation is not necessarily the progenitor of the cluster spin SG. Instead, we believe that the spin distortions generated by the holes and the Sr disorder are the key aspects of this problem.

A summary of our theoretical and experimental results for this spin texture follows:

(i) Clusters of antiferromagnetically correlated regions are formed, the boundaries of which are defined by the Sr impurities. These domains have AFM order parameters which vary in direction, and thus long-ranged AFM order in this doping regime is destroyed by the lack of orientational order of the moments of these clusters. The smallest collection of impurities which forms a small cluster of AFM correlated spins is three noncolinear Sr impurities, and from such three-impurity configurations it is established that domain walls separating the clusters are regions of disordered spins which have a larger local ferromagnetic (FM) correlation than anywhere else in the lattice. Also, since carriers are much more mobile in FM regions, it is reasonable to assume that this spin texture leads to meandering rivers of charge connecting the impurity sites — namely, at the higher temperatures at which the holes move the domain walls constrain and are populated with the mobile holes. This spin texture thus explains why the $x \lesssim 0.05$ material does not develop incommensurate magnetic fluctuations: since the holes are ''expelled'' from the AFM clusters by their preference for moving in a FM region, there is no impetus for the local magnetic order to peak at any wave vector other than $\mathbf{Q}=(\pi,\pi)$. We demonstrate this for the low-temperature spin texture by the explicit evaluation of $S(\mathrm{Q})$.

(ii) (a) The susceptibility experiments of Chou *et al.* on the SG phase of $La_{1.96}Sr_{0.04}CuO_4$ between 20 and 100 K displayed an anomalously small Curie constant.[6] We have grown a new set of samples using the traveling-solvent, float-zone method, for a variety of concentrations in the SG regime. We have determined the Curie constants for all of these samples, and have determined how this constant changes with doping concentration in the SG phase.

(b) Modeling the topology of the SG phase in terms of small domains of AFM correlated spins separated by disordered domain walls, and then treating the clusters as independent low-spin magnetic units, we show that such a small moment follows immediately, and that it increases with doping by one over the correlation length squared. This result is in quantitative agreement with experiment, and thus our comprehensive experimental study of this quantity serves as a critical test of the cluster SG phenomenology.

(iii) As mentioned previously, this model accounts for some observations in the AFM phase, and in this paper we show that it also describes some results found in the SG phase. If this model is an accurate representation of the spin texture in all doping regimes it should also be able to explain the appearance of incommensurate correlations for $x \approx 0.05$.[16] Indeed, we find that this is the case, providing very strong support for this model. We associate this phenomenon with the degradation of the integrity of the domains of the cluster SG as doping levels are increased, and relate the delay in the appearance of the incommensurate correlations to impurity disorder effects. We propose that our results are suggestive that the mechanism behind the incommensurate phase follows from the spiral phase theory of Shraiman and Siggia.[17]

Our paper is organized as follows. First, in Sec. II we discuss our model of the spin distortions introduced by a single Sr impurity and a single hole, and explain how this may be used to study the effects of a nonzero density of holes all localized around Sr impurities. Then we present an analysis of a small number of Sr impurities (three, in fact) that leads to an understanding of how domains of AFM correlated spins are produced, and survey results from our extensive numerical simulations that produce the ground states

for our model Hamiltonian. In Sec. III we present new experimental results for the susceptibilities of this compound just above the SG transition temperature, and then show how the above-mentioned small AFM domains adequately describe the observed Curie constants. In Sec. IV we present a discussion of the commensurate-to-incommensurate transition, and relate the effects of spin distortions that we have included explicitly to theoretical mechanisms for the spiral phase. Last, we summarize our results and relate them to other outstanding problems in the study of moderately doped LaSrCuO. A brief, preliminary report on this work has already appeared elsewhere.[18]

II. MODEL AND SIMULATION RESULTS

A. Model Hamiltonian for a single hole around a Sr impurity

It is well known that the near-neighbor Heisenberg Hamiltonian provides a very accurate representation of the magnetic properties of the 2D CuO_2 planes[19,2] apart from small anisotropies which we ignore in the present paper (e.g., these anisotropies only affect the correlation length when it becomes of the order of 80 lattice constants, a distance that greatly exceeds any length scale discussed in this paper). Thus, we represent the magnetic interactions between the Cu spins using

$$H_J = J \sum_{<ij>} \mathbf{S}_i \cdot \mathbf{S}_j , \tag{2}$$

where $\langle ij \rangle$ denote neighboring Cu sites, and J is the exchange constant, known to be of the order of 1550 K.

At low doping levels and at low temperatures, transport measurements[13,7,14] suggest that the carriers move by hopping. Presumably their motion corresponds to the holes hopping from one impurity site to another, such as occurs in doped semiconductors before the metal-nonmetal transition. Then, it is appropriate to consider the response of the magnetic background to carriers localized in the vicinity of the Sr impurity ions. A variety of previous theoretical studies[9,20,21] have all shown that the ground state for a single hole in such a situation corresponds to a doubly degenerate ground state for which the hole circulates either clockwise or counterclockwise in the plaquette directly above or directly below the Sr impurity. The hole motion couples to the transverse fluctuations of the Cu spins and produces a spiraling twisting of the AFM order parameter,[9,22] a state that is topologically similar to the singly charged skyrmion excitations of the 2D classical nonlinear σ model.[23]

One of us and Mailhot[10] proposed that a simple way of representing the effects of this circulating hole motion on the AFM background was to integrate out the hole motion and replace it by a purely magnetic interaction. For (1,2,3,4) denoting the four spins in the plaquette bordering the Sr impurity, the interaction Hamiltonian for a single hole is given by

$$H_{\rm int} = -\frac{D}{S^4}[(\mathbf{S}_1 \cdot \mathbf{S}_2 \times \mathbf{S}_3)^2 + (\mathbf{S}_2 \cdot \mathbf{S}_3 \times \mathbf{S}_4)^2 + (\mathbf{S}_3 \cdot \mathbf{S}_4 \times \mathbf{S}_1)^2 + (\mathbf{S}_4 \cdot \mathbf{S}_1 \times \mathbf{S}_2)^2]. \tag{3}$$

One may show that for classical spins, as long as $D/J > 2.2$ the ground state of $H_J + H_{\rm int}$ has the same topology as that of the circulating hole ground state. The factor of S^4 ensures that this Hamiltonian scales as S^2, the same as the near-neighbor Heisenberg Hamiltonian (which facilitates the inclusion of quantum fluctuations in a straightforward manner), and the ratio $D/J \approx 3$ has been suggested[10] on the basis of (i) comparisons to Raman scattering results and (ii) a numerical simulation that has been shown to be consistent with Eq. (1). From now on we shall assume that this interaction Hamiltonian represents the spin texture in the neighborhood of any Sr impurity, and that we can represent the low-temperature multiply doped state with such an interaction present at every plaquette bordering a Sr site.

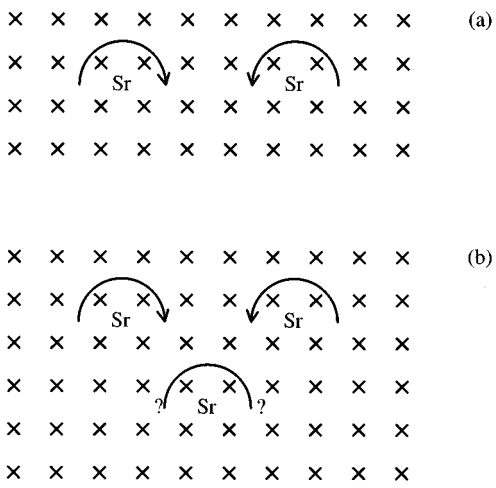

FIG. 1. (a) A schematic of the interaction between competing circulations for two Sr impurity sites. When the chiralities of these states are opposite, one finds that the currents add in a constructive fashion. This is the ground state for any two impurities. (b) If one adds a third noncollinear Sr impurity to the previous situation, neither a positive nor negative circulation for the third impurity leads to only constructive current interactions, and thus this situation is frustrated.

B. Impurity state interactions

One may examine the interaction between pairs of these skyrmionlike impurity states and explain the transverse spin-freezing temperature found experimentally.[11,12] In this section we wish to consider the interactions between more than two such impurity states, as this immediately leads one to an understanding of the possible origin of the cluster spin glass phase.

Around each impurity site the ground state is chiral, with the spin distortions corresponding to either clockwise or counterclockwise circulations. On the basis of only this fact it is straightforward to predict the ground state for two Sr impurities: as shown in Fig. 1(a), if one chooses opposite chiralities around the two Sr sites, then the ''currents'' (either those of the motion of the hole, or the concomitant spin currents—see Ref. 10) add constructively in the region between the impurities. One may show, either numerically or analytically, that this is indeed the ground state. Now consider three noncollinear Sr impurities. It is clear that there is no configuration for which the chiralities assigned to each impurity do not destructively interfere with one another—

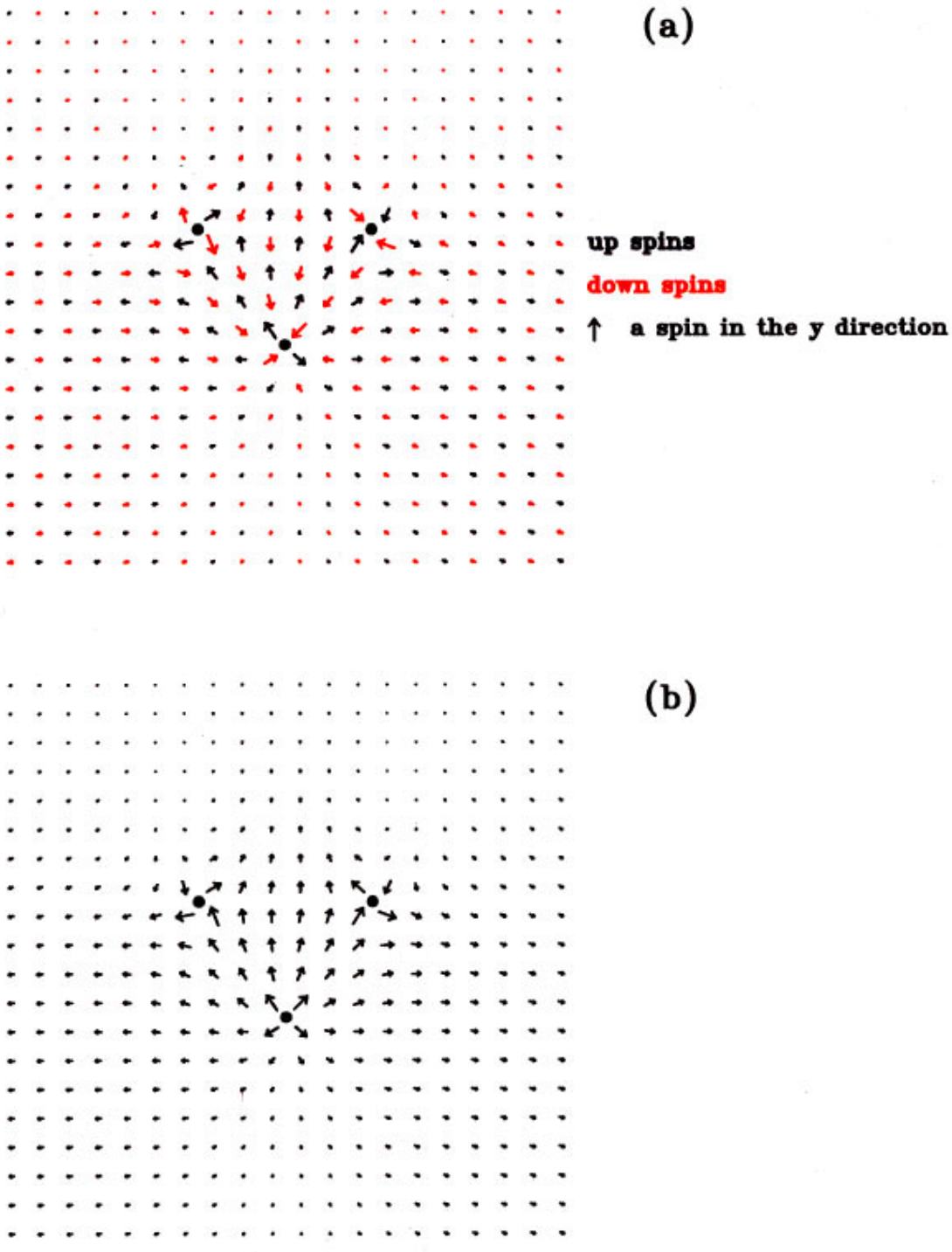

FIG. 2. (Color) (a) The distribution of spin directions for the ground state surrounding three noncollinear Sr impurities (indicated by solid circles). What is shown is the projection of a spin's direction onto the plane of the paper (to aid in the understanding of these figures, a spin lying entirely in the page pointing to the top of the page is shown at the right). Then, the blue spins represent those spins pointing up out of the page, while the red spins represent those spins pointing below the page. (b) The same as in (a) with the *B* sublattice spins flipped (such that an AFM would appear as a FM). This aids in the visualization of the spin directions, and more directly shows how the orientation of the AFM order parameter in the domain formed by the three Sr impurities (lying approximately in the plane of the page pointing to the top of the page) is rotated with respect to the direction of the AFM order parameter in the bulk of the lattice, the latter pointing directly up out of the page.

three such impurity states necessarily lead to a frustrated interaction between the spin distortions created by each Sr impurity, as shown in Fig. 1(b), and the question then arises: what is the ground state of this configuration of impurity sites?

Figure 2 shows the ground state that we have found (our method for finding the ground state is detailed in the next subsection[24]) for three impurity sites placed in the positions of an isosceles triangle with the lengths of the sides roughly equivalent to the separations between randomly placed Sr

impurities for a doping level in the middle of the SG phase. Figure 2(a) shows the actual spin directions, whereas Fig. 2(b) shows the spins on all B sublattice sites flipped, as this substantially improves the visualization. The Hamiltonian is isotropic in spin space, and thus we have complete freedom to orient the spins in any direction — we have chosen that the AFM order parameter would point directly out of the page infinitely far from these impurities.

Figure 2(b) most clearly shows the very important result that the state that is produced by the frustrated current interactions is a small domain of AFM correlated spins whose orientation is rotated with respect to that of the bulk AFM. For example, in the configuration depicted in the figures the domain's AFM order parameter points toward the top of the page whereas the order parameter of the bulk AFM points out of the page. Also, there are narrow domain walls separating this domain from the bulk of the lattice, although as expected theoretically[10,22] the spins distortions decay algebraically as one moves away from the Sr impurities. With many Sr impurities distributed randomly above and below a plane, we thus expect to find many such domains, and we now analyze the results from our numerical determination of the ground states showing that this is indeed an appropriate way to think of this phase: these domains are the predominant components of the cluster SG spin texture.

C. Ground state spin textures for the SG regime

As explained above, the ground state for a random distribution of Sr impurities is frustrated (viz., the interactions between impurities are frustrated). Thus, standard numerical approaches such as the conjugate-gradient method usually find low-lying states, but not the ground state. We have numerically searched for the true ground states using a technique first put forward to examine a random distribution of frustrating FM bonds doped into a 2D AFM XY model on a square lattice,[25] a technique that from now on we shall refer to as the Grempel algorithm. This approach was formulated after earlier work[26] showed that the lower energy states of this latter model could be thought of in terms of small domains of AFM correlated spins separated by domain walls, very similar to the spin texture that we are proposing for our perturbed Heisenberg model.

Given that the Grempel algorithm is helpful in illuminating the physics of the cluster SG phase, we briefly explain its key features with regards to the Sr impurity problem discussed in this paper. First, for a given lattice size and distribution of the Sr impurities we start by assigning random directions to all spins. Then, using the conjugate-gradient technique we ''relax'' the system and find a state that is a local minimum on the SG energy surface. We repeat this for up to fifteen initial conditions (our results did not change when we experimented and used more than fifteen). Then, we applied the Grempel algorithm to find lower energy configurations: We begin with the lowest-energy relaxed state and first calculate the local field at each lattice site, the latter being defined by

$$\mathbf{H}_i = \sum_{j \epsilon \langle ij \rangle} (-1)^j \mathbf{S}_j . \tag{4}$$

(Although $\mathbf{H}_i$ is not the exact local field for the spins on the Sr-doped plaquettes, it nonetheless supplies an adequate description of the disorder and frustration in the spin morphology.) If these classical spins are assumed to be of a unit magnitude, then the maximum magnitude of the local field is 4. Then we calculate the local field's magnitude for each spin, and if it is lower than some critical field H^*, we change its orientation to be any direction. For those sites which have a large local field, only a small random angle is used (chosen from no more than 5% of the 4 π steradians on the unit sphere). This method ensures that large domains of AFM correlated spins have their integrity preserved at this step, whereas the domain walls, the regions of more strongly disordered spins (and thus smaller local fields), are allowed to more fully explore the full spectrum of spin directions. Then, another local minimum is found using the conjugate gradient method and the Grempel algorithm is repeated with this new local minimum. This procedure allows the system to more easily access its lower energy states. We have varied the critical field H^* from 2 up to 3.9 after each application of the conjugate gradient method, and find that after only 3 or 4 applications of the Grempel algorithm the (presumably) true ground state is found. A full critique of the success of this method may be found in Ref. 25.

We have found ground states (or at the very least, very low-energy states) for Sr doping concentrations corresponding to values of $x = 0.02, 0.035, 0.05, 0.065$, and 0.08. Different lattice sizes, $L \times L$ with $L = 20$, 30, 40, 50, and 60, and different distributions of Sr impurities, at least five for each x, are implemented as described in the Appendix. In order to obtain better statistics we also included 80×80 clusters for $x = 0.02$ and $x = 0.035$. (We impose one restriction on each distribution of Sr impurities—in an attempt to mimic the Coulomb repulsion between impurities that would tend to force them apart during the crystal growth process, we do not allow for two near-neighbor plaquettes both to contain Sr impurities.)

As a check that we are indeed finding ground states consistent with the actual spin texture of LaSrCuO, from these ground states we obtained the following quantities: (i) The bulk value of the staggered magnetization. Assuming that the finite-size scaling for the staggered magnetization is the same as it is for the undoped lattice *if* the system possesses long-ranged order,[30] viz., $M^{\dagger}(L) \sim M^{\dagger}(\infty) + O(1/L)$, we find that for $x = 0.035 \rightarrow 0.08$ long-ranged order is absent; for $x = 0.02$ finite-size effects are too large for us to determine if long-ranged order is present. Thus, it is unclear whether or not our $x = 0.02$ simulations are properly reflecting the absence of long-ranged AFM order found experimentally[12] for $x \geq x_c = 0.0175 \pm 0.0025$. (ii) The zero temperature correlation length vs doping. We have used the finite-size scaling ideas that are covered in the Appendix to extract this quantity from our ground states. Our results are shown in Fig. 3, along with a compilation of all two-axis experimental data. Clearly, over the $0.035 \leqslant x \leqslant 0.08$ range of doping our numerically determined correlation lengths agree with experiment quite well. For $x = 0.02$ we find a correlation length that is significantly less than the approximately 40 lattice constants found in the experiments of Keimer *et al.*[7] The possible reasons behind this failure are similar to those discussed above: For such a large correlation length we would

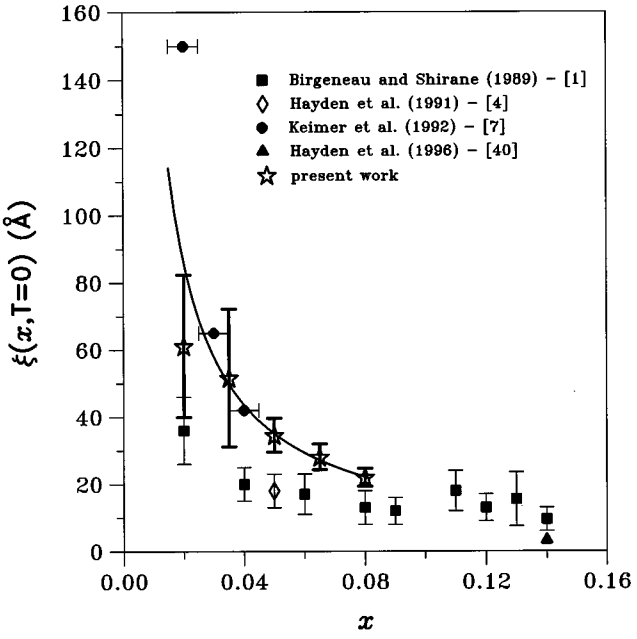

FIG. 3. The correlation length determined from our ground states as a function of x at $T=0$ (the open stars) in comparison to all of the two-axis neutron-scattering data collected since 1989 (from the collection of data in Ref. 2) with the reference numbers included inside of angular brackets. The solid line is the fit of our data to the expression given in Eq. (5) with $A=0.49$ and $\beta=0.98$, and shows how well this empirical form fits both our numerical results and the 3 and 4 % samples studied in Ref. 7.

have to study systems that were of a linear dimension that were at the very minimum twice the correlation length. Also, because of the low concentration, the average should be over more distributions of disorder to properly sample what a low concentration bulk system would be like. Thus, for the $x=0.02$ simulations both finite-size effects and a restricted averaging over disorder potentially limit the reliability of our simulations and thus prevent a proper comparison with experiment. We have been able to fit our $\xi(x,T=0)$ data for $x\geqslant 0.035$ to the following empirical form (setting the lattice constant to be one from now on):

$$\xi(x,T=0)=\frac{A}{(x-x_c)^{\eta}}\,. \tag{5}$$

We find that the best fit occurs for $A\sim 0.49$, $x_c=0.0$, and $\eta\sim 0.98$, and thus our data are reasonably consistent with the scaling $\xi(x,T=0)\propto 1/x$. This implies the vanishing of long-ranged AFM order in the plane at $T=0$ for any nonzero density of Sr impurities, a result that may be understood in terms of the algebraic decay of the spin distortions produced by a single hole localized near a Sr impurity. The resulting curve is shown in Fig. 3, and clearly represents a good fit to both our numerical data and the data found in the study of the $x=0.03$ and 0.04 samples by Keimer *et al.*[7]

The $x=0.02$ results described in the two points listed above suggest that, due to finite-size effects, we are unable to reliably simulate the $x=0.02$ phase, and thus from now on we focus on samples with a minimum concentration of $x=0.035$.

Encouraged by the $x\geqslant 0.035$ successes, we now describe the spin texture, at a microscopic level, that is associated with these ground states. We proceed in a manner that most clearly displays the existence of the domains. The first information that details the kind of inhomogeneous spin texture that exists in the SG phase is the local field defined in Eq. (4). In Fig. 4(a) we show the local fields for an $x=0.035$ distribution of Sr impurities (this concentration is in the middle of the SG phase) on a 60×60 lattice. The plaquettes having a Sr impurity above or below them are shown as open squares, and the size of the local field at the Cu sites is indicated by the radius of a solid circle. For this figure all local fields less than 99% of the maximum local field are not included. (Smaller values of this field do not affect the qualitative features of this figure: the domain wall widths become smaller and the continuity of the domain walls connecting neighboing Sr sites is not as clear, so here we use this relatively large local field to make the domain walls' appearance as obvious as possible.) This figure displays some evidence of clusters of strongly AFM correlated spins; clearly, some regions of spins are no longer strongly AFM correlated with other regions. However, what this figure most clearly shows is that there are channels of disordered spins (defined as having a reduced local field) that are set up connecting neighboring Sr impurities—these paths of disordered spins are the domain walls of the clusters.

More complete information concerning the actual spin texture that is found follows from the kind of figure shown in Fig. 4(b). This diagram corresponds to the same ground state shown in Fig. 4(a), and is constructed in the same way as Fig. 2—the projection of each spin onto the xy plane is shown, and every spin on a B sublattice site is flipped so that a completely ordered state would appear to be a FM state with all spins pointing up out of the page. A careful examination of this figure clearly shows the existence of the domains. For example, in the upper middle portion of this figure a region bounded by six Sr impurities is seen to produce a domain of strongly AFM correlated spins. Further, one may characterize the sizes of the domains using figures such as Fig. 4(b)—we have done this for a number of the ground states found in 60×60 lattices, and observed that the average number of spins per domain varies as $\xi(x,T=0)^2$ to within 10%.

Many other examples of these domains can be found, some being three, four, . . . , sided domains. These assemblies are always associated with the Sr impurities being at the edges of the clusters, and thus it is clear that these AFM correlated regions are a result of the dopant disorder. It is the domainlike spin texture of this phase which motivates us to refer to it as a cluster SG.

One question that this spin texture answers is the elimination of long-ranged AFM order: we find that the orientations of the local AFM order parameters of these clusters is random, and thus the disappearance of AFM order may be thought of in terms of the lack of orientational order of the local cluster moments. Thus, the long-ranged AFM order is replaced by the SG order.

D. Commensurability of the spin correlations in the SG phase

One may calculate $S(\mathbf{Q})$ for the ground states of the $x=0.02$ or $x=0.035$ states, and it is always found that the

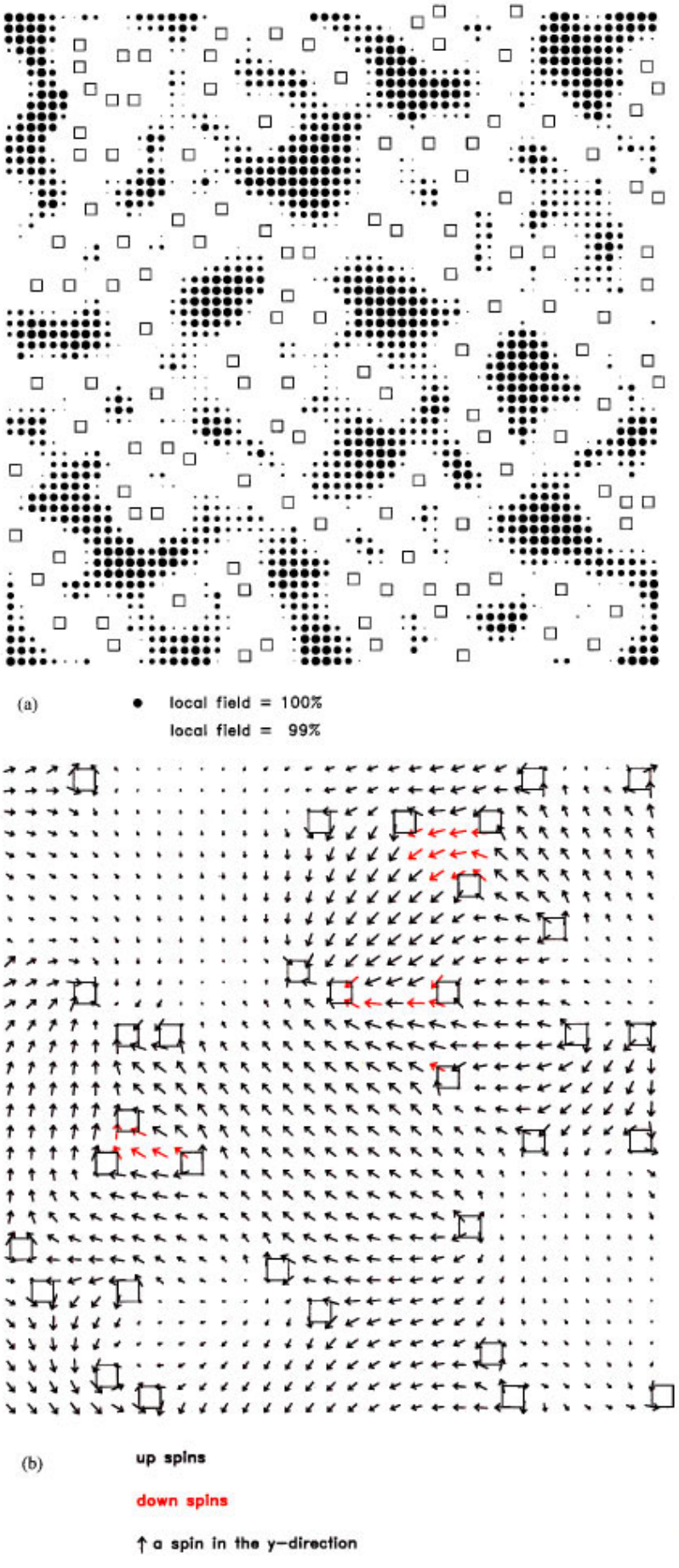

FIG. 4. These pictures explain the spin texture of a $x=0.035$ system for one particular distribution of Sr impurities on a 60×60 lattice. The plaquettes containing Sr impurities are shown as squares. In (a) the local fields, as defined in Eq. (4), are shown. Clusters of various sizes and shapes are seen, but the most striking feature of this picture is the presence of percolating paths of disordered spins (viz., spins that are not antiferromagnetically correlated) that connect the Sr impurities. In (b) (Color) the projection of the spins in the middle of this lattice (a 30×30 region) onto the plane of the page is shown, similar to the construction in Fig. 2(b) (wherein the spins on a B sublattice site are flipped).

peak occurs at the commensurate AFM wave vector $\mathbf{Q}=(\pi,\pi)$. (For higher doping concentrations incommensurate correlations develop, a subject that we shall discuss in Sec. IV.) This is consistent with the experimental observation that the spin correlations remain commensurate in the SG phase.[7,16] To see that this may still be the case even if the holes are mobile simply note that holes like to move in FM regions rather than AFM ones. Then, since the domain walls are more disordered than the interior of the domains, they necessarily have a greater FM correlation present; thus, the holes will tend to move along the domain walls. Put another way, the holes are *expelled* from the interiors of the domains, and only move along the domain walls. (A complete theoretical discussion of the transport in the low x compounds will be presented elsewhere.[14]) This provides a plausible explanation of why the spin correlations remain commensurate both at low temperatures, when the hole's motion is dominated by the Sr impurity potentials, or at higher temperatures, where the holes are mobile (and a resistivity that varies linearly with T is found). We note that a similar explanation of the commensurability of the SG phase was pointed out by Emery and Kivelson.[15]

III. CURIE CONSTANT

An important experimental result contained in the study of Ref. 6 involves the behavior of the susceptibility vs temperature just above the SG transition temperature, T_G. To be specific, $T_G \approx 10$ K and it was found that from roughly 20 to 100 K the susceptibility $\mathcal{X}(T)$ could be described via a Curie form with the Weiss constant equal to zero,

$$\mathcal{X}(T)=\mathcal{X}_0+\frac{\mathcal{C}}{T}. \tag{6}$$

For one well-studied $x=0.04$ sample it was found that the Curie constant $\mathcal{C}$ was very small, corresponding to only 0.5% of the Cu spins present in the sample. Other samples studied in the work associated with Ref. 6 were found to have similar susceptibilities with Curie constants corresponding to between 0.2 and 4 % of the Cu spins present in the sample.[27] In this section we present experimental results that detail the manner in which $\mathcal{C}$ varies with doping level, and then show how the spin texture described at the end of the previous section leads to a straightforward and plausible explanation of this behavior.

A. New experimental results

Single crystals of $La_{2-x}Sr_xCuO_4$ (x = 0.02, 0.025, 0.035, and 0.045) of masses around 2.0 g have been grown using a crucible-free, contamination-free, traveling-solvent floating zone (TSFZ) method.[28] The stoichiometric feed rods are prepared from the proportional amount of high purity originals ($>$99.999%) La_2O_3, $SrCO_3$, and CuO. The solvent rods are prepared using CuO as self-flux (20% La_2O_3, 80% CuO). The optical floating-zone furnace uses four elliptical mirrors with halogen lamps at one focal point and the solvent zone is melted at the second focal point. The growth rate is about 1 mm/h, the rotation rate is 50 rpm opposite, and the growth is done under air flow.

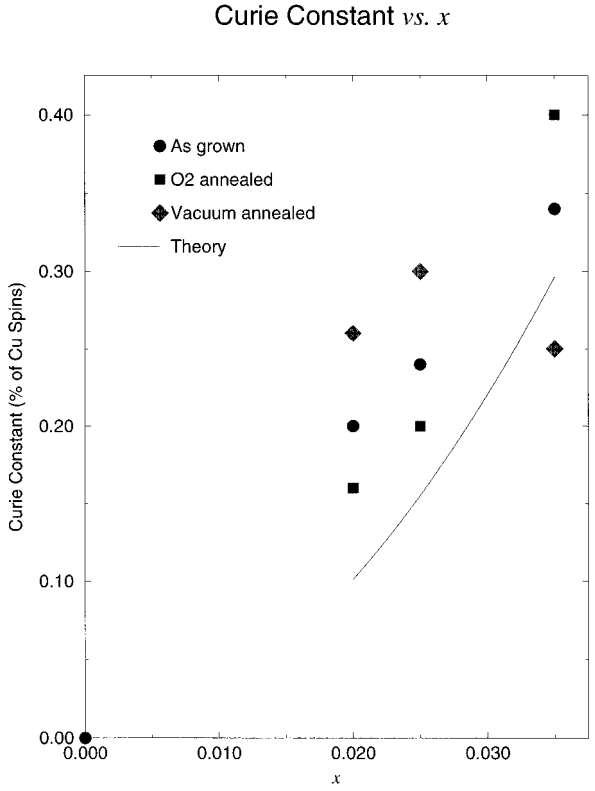

FIG. 5. The variation of the effective Curie constant, expressed as a percentage of the contribution that would arise from independent $S=1/2$ ions with $g=2$ at each Cu site, for several different LaSrCuO samples vs x. The theoretical prediction contained in Eq. (7), using the correlation length expression given in Eq. (5), is also shown.

The as-grown single-crystal samples were prepared using identical preparation techniques—it was hoped that this would produce a reliable trend of the Curie constant with doping (see below). For the first three concentrations, this was the case. Unfortunately, the $x=0.045$ sample showed signs of superconductivity, and this concentration will only be addressed in the next section. The as-grown crystals were subsequently exposed to additional treatments: oxygen annealing or vacuum annealing. The oxygen annealing was performed at a temperature of 600 °C for 10 h. The vacuum annealing has been done at 850 °C under $\approx 10^{-6}$ Torr for one hour. The susceptibility results for these samples were very similar to those of the as-grown samples, thus supporting our contention that these are excellent single crystals with a high degree of Sr impurity homogeneity.

The magnetization as a function of temperature has been measured using a Quantum Design superconducting quantum interference device magnetometer. The M vs H data indicate that there are no ferromagnetic impurities present within our instrumental resolution. The obtained M vs T data were replotted as $\mathcal{X}T$ vs T to extract the Curie constants from the region above T_G in which the slope is a constant.

The data for our samples are presented in Fig. 5; the 0.5% value for the Curie constant quoted for the $x=0.04$ crystal studied in Ref. 6 is similar to that extracted from this figure. The Curie constant is expressed as follows: for a given mass of LaSrCuO we calculate the Curie constant that would be

expected if all of the Cu spins were isolated $S=1/2$ spins with $g=2$, and call this $\mathcal{C}_0$. Then, we express the Curie constant found in the region above T_G as a fraction of $\mathcal{C}_0$. The errors in our data are roughly constant and equal to 10% of the measured values.

In the as-grown samples there is a clear indication of a linear variation with doping concentration, approximately given by $\mathcal{C}(x)/\mathcal{C}_0=(0.1\pm0.02)x$. For the O_2 annealed samples it could be argued that the Curie constant grows quadratically with doping, whereas for the vacuum annealed samples it appears that the Curie constant is nearly independent of x (we note, however, that the oxygen depletion is expected to be largest for the higher Sr dopings for vacuum annealing, and thus our identification of hole doping levels with x is least accurate for this preparation technique). Despite this variation, it is pleasing that in all cases the magnitude of the Curie constant is roughly similar, and we now present a heuristic argument that accurately tracks this behavior.

B. Cluster SG model of the Curie constant

The results from the work of Sec. II C suggested that the spin texture of the low-temperature moderately doped LaSrCuO system can be thought of in terms of small clusters of AFM correlated spins separated by narrow domain walls of disordered spins. The linear dimension of these domains tracks the zero-temperature correlation length. Also, in the above section we showed how the Curie constant found in the temperature range just above T_G varied with x, with an anomalously small number of effective Cu spins contributing to this constant. In this section we show that these two results are compatible with one another, and thus establish the consistency between phenomenologies promoting the existence of a cluster SG[4,5] and the experiments that showed that this material has a canonical SG phase.[6]

We describe the cluster SG spin arrangements in terms of domains of spins, the sizes of the domains corresponding, on average, to the zero-temperature correlation length, and narrow domain walls composed of strongly disordered spins. Due to the domain walls we make the assumption that there is no interaction between the domains — this is consistent with the vanishing Weiss constant found experimentally. Then, the effective Curie constant for this spin texture follows immediately: as a simple picture of such spin configurations, let each domain be of a $L\times L$ geometry; further, take $L\sim\xi(x,T=0)$. Noting that the quantum-mechanical ground state for such a cluster is a $S=0$ singlet for L even, and a $S=\frac{1}{2}$ doublet for L odd, *and* that the gaps to the first excited states are large,[29] as a first approximation we take the singlet clusters to be magnetically inert (in the temperature interval over which the susceptibility was measured). Accordingly, for a lattice with N Cu spins, the susceptibility arises from $N/(2L^2)$ spin-$\frac{1}{2}$ magnetic units. Finally, for a cluster SG we predict

$$\frac{\mathcal{C}}{\mathcal{C}_0}\sim\frac{1}{2\xi^2}. \tag{7}$$

The result of using Eq. (5) for the correlation length is also shown on Fig. 5, and displays the quantitative agreement between this admittedly highly simplified theory and experiment. Given that we have ignored any contribution from the domain walls, it is not surprising that our value for the Curie constant is somewhat less than what is observed experimentally. Further, Eqs. (5) and (7) together approximately yield $\mathcal{C}/\mathcal{C}_0\propto x^2$, consistent with the overall trend of an increasing Curie constant with x.

IV. INCOMMENSURABILITY vs DOPING

In *all* ground states we have found some evidence for domains. These clusters are antiferromagnetically correlated, so it is not surprising that in the SG phase we found that the dominant magnetic correlations are commensurate, as we described in Sec. II D. However, as x increases we find that the areal fraction associated with the domain walls starts to dominate at the expense of the clusters, and thus the persistence of AFM correlations is no longer guaranteed. This is shown most clearly in Fig. 6 wherein we show an $x=0.08$ result for the local fields — the $x=0.035$ result for the same distribution of Sr impurities (at a lower concentration — see the Appendix) is shown in Fig. 4(a). As is seen from a comparison of these two figures, the concept of domain walls is lost: only in a small number of regions can one say that there are any clusters, and thus the concept of domain walls separating the clusters is irrelevant. Instead, almost everywhere there is a more homogeneously distorted spin texture, and effectively dopant disorder is being averaged out. This is consistent with the experimental result[16] that for $x=0.06$ one only observes the Curie behavior over a much smaller temperature range ($20\leqslant T\leqslant 50$ K), and the Curie constant that is found is much smaller, whereas for higher x no Curie-like behavior is found at any temperature. We now consider this behavior in relation to the observed commensurate-incommensurate transition.

Recent experimental work by Yamada *et al.*[16] has shown that the incommensurate (IC) correlations found in more strongly doped LaSrCuO (Refs. 31–34) develops continuously as the Sr doping concentration is increased, with a critical concentration corresponding to $x_{IC}\approx 0.05$. It is very intriguing that these correlations first develop at the x value for which superconductivity first appears, and thus makes the mechanism behind the appearance of the IC phase an important question. Here we show that our model, based on spin distortions produced by holes localized around Sr impurities at low temperatures, reproduces this commensurate-incommensurate transition. Most importantly, any model of mobile holes that induces spin distortions analogous to those discussed here may also produce a similar IC phase, and it can be argued[10] that what we are analyzing are ''snapshots'' of the kinds of effects produced by mobile holes generating dipolar backflow spin distortions.

We have only calculated the ground-state spin textures for this system. Thus, we cannot directly compare our results to the measured dynamic structure factors $\mathcal{X}''(\mathbf{Q},\omega)$ found experimentally. Instead, we examine $S(\mathbf{Q})$, and look for signs of incommensurate correlations in the snapshots of the ground state spin texture.

We find that at $x=0.05$ two of the five distributions of Sr impurities generate IC correlations. For $x=0.065$ three of the five distributions generate IC correlations, whereas for

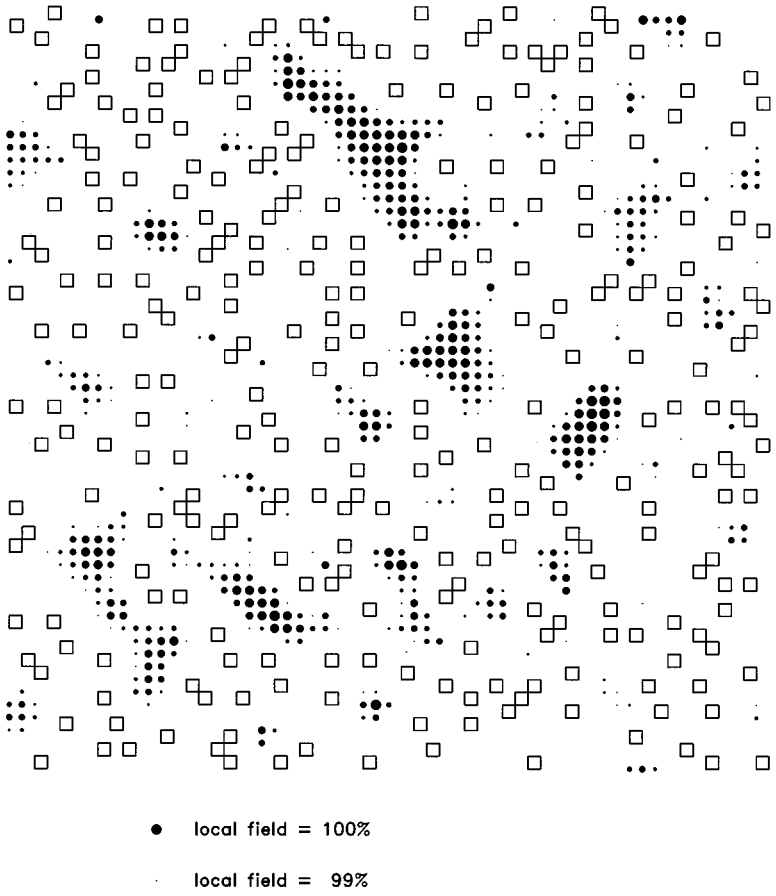

FIG. 6. The same as Fig. 4(a) for $x=0.08$. There are fewer clusters present in this ground state, and instead this spin texture is found to be much more homogeneous. Such a state has a Curie constant that is much smaller than that predicted by Eq. (7) due to the absence of clusters. This behavior is consistent with experiment.

$x=0.08$ all five of the distributions of Sr impurities generated IC correlations. From these numbers we conclude that the C-IC is seemingly continuous and happens close to $x\sim 0.06$. This number is very close to that found experimentally. Also, in *both* experiment and our simulations the correlations develop along $(\pm 1,0)$ or $(0,\pm 1)$. This agreement between our work and experiment is striking, and suggests that mechanisms which produce the IC phase by spin distortions, such as the spiral phase mechanism of Shraiman and Siggia,[17] should be reexamined with an eye to understanding the stability of this phase in the presence of strong Sr impurity disorder (albeit with a bias towards maximum hole density around the Sr impurities).

V. SUMMARY

We have considered a simple model of the effect of holes at low temperatures that are localized around the Sr impurities in LaSrCuO and have found evidence for clusters of AFM correlated spins in the SG phase — we believe that this spin texture provides ample reason to refer to this state as a cluster SG. That this twofold degenerate chiral ground state leads to a SG phase lends support to the prescient speculations of Villain.[35] We briefly note that we have also considered another related model of spin distortions produced by localized O holes, the so-called Aharony model, and we still find strong evidence for such clusters in this model of Sr impurity disorder. Thus, our result is seemingly model independent *providing* that the Sr disorder is included explicitly.

We have examined in greater detail, using new TSFZ grown crystals, the anomalously small Curie constant that was measured in Ref. 6, and have characterized both its magnitude and the manner in which this constant changes with doping. We have thereby provided a quantitatively accurate model of this Curie constant by utilizing the idea that the clusters behave like independent low-spin quantum units.

We have also shown that the C-IC transition in our model is continuous, and occurs at roughly the same x as is found experimentally. We thus attribute the critical value of $x_{\rm IC}$ to Sr impurity disorder. Also, our model induces incommensurability in the same axial directions $[(\pm 1,0),(0,\pm 1)]$ as is found experimentally. Given that the spin distortions produced by the partially localized holes studied in this paper are similar to the dipolar backflow spin distortions induced by mobile holes in the theories of Shraiman and Siggia, it is possible that a model of such holes including the effects of Sr disorder for $T\gg T_G$ will provide an accurate representation of the physics of the intermediately doped LaSrCuO system studied here. We note that previous theoretical claims of an incipient phase separation of the spiral phase must be reinvestigated using a model that includes explicitly the Sr disorder; it is likely that disorder will completely suppress this instability. We will report on the results of related studies in a future publication.

In none of the theoretical work presented here have we included the quantum fluctuations of the Cu spins, instead relying on a classical model of the spins. Support for this idea follows in part from the success of the renormalized classical model in describing the undoped phase. However, we are now utilizing inhomogeneous, linearized, spin-wave

theory, including the modified spin-wave theory constraint to enforce the fact that there is no long-ranged order in the SG phase, to assess the importance of quantum fluctuations to these results. Further, upon completion of these results, we should better be able to test if the dynamical fluctuations of such a cluster SG phase are responsible for the unusual scaling of $X_T''(\omega)$ found by Keimer *et al.*[7]

We have also not included the XY anisotropy, a component that could possibly affect our results. However, the topology of a cluster SG was first found in a 2D XY model,[26,25] and thus it seems highly unlikely that this small interaction would qualitatively affect our conclusions, especially given the small AFM correlation length in the SG phase. Other magnetic anisotropies would serve to sharpen the domain walls separating the clusters, and thus could only serve to strengthen our arguments.

Last, we note that the ideas expressed in this paper are not necessarily limited to the Sr-doped 214 compound. Recent work by Budnick *et al.*,[36] has shown that Sr-doped 123 (with the Sr substituting for the Y ions) produces a similar SG phase, and by symmetry we expect similar impurity ground states in this material. Also, Li-doped 214, studied originally by Endoh *et al.*,[37] and more recently examined in Ref. 38, potentially has chiral impurity states, as recently discussed by Haas *et al.*[39] So, it is possible that similar physics might also be found in this compound.

Note added in proof. We have performed numerical determinations of the ground state for $x=0.02$ for five different impurity distributions for 100×100 clusters, and have thus confirmed the absence of long-ranged AFM order for this Sr doping level.

ACKNOWLEDGMENTS

We wish to thank David Johnston for providing us with a collection of the measured correlation lengths, and for other valuable comments. We also wish to thank Barry Wells, Martin Greven, Marc Kastner, Pakwo Leung, and Ferdinando Borsa for helpful comments. This work was initiated while one of us (R.J.G.) was visiting MIT, and he wishes to thank them for their warm hospitality. This work was supported by the NSF, Grant No. 93-15715 and by the NSERC of Canada.

APPENDIX

One of the outstanding problems of theoretical solid-state physics involves the determination of accurate finite-size scaling forms for disordered systems. We have attempted to circumvent this problem in the following manner: we have performed our numerical simulations of this spatially disordered system by imagining that we have $\mathcal{N}$ large samples of the crystal, all having the same average density of Sr impurities above and below a CuO_2 plane. Then, for one of the $\mathcal{N}$ large samples, choose some square subsystem of the sample of dimension $L_1\times L_1$, and find its ground-state spin texture. Then, as schematically shown in Fig. 7, we have studied increasingly larger subsystems, namely $L_2\times L_2$ and then $L_3\times L_3$, etc., with $L_1<L_2<L_3\cdots$ that include exactly the same distribution of impurities in the smaller subsystems as are present in the larger subsystems. Then, as one increases the density of Sr impurities we add more impurities to the initial distribution to raise x to the desired value. From such sets of data we have found that we can best obtain good statistics for each sample, and then we perform an average over all $\mathcal{N}$ samples. Further, the manner in which we increase the density of impurities leads to smoother variations of quantities with x. We repeat this process for a number of differing initial, low density distributions of impurities, and we find that quantities like the correlation length are very well converged with only five samples per x.

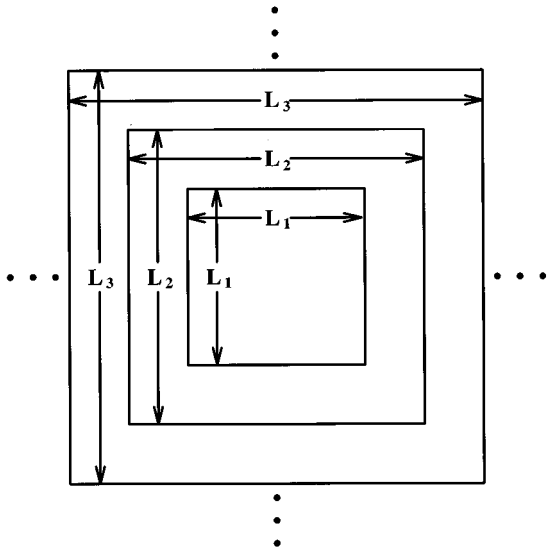

FIG. 7. This figure shows smaller lattices embedded in larger lattices. The idea behind this construction is that what we want to study is small chunks of an infinite system, and see how one approaches the infinite system by taking larger and larger sections. Since we are considering a disordered system, translational periodicity is broken and we must make sure that the larger clusters contain the same distribution of impurities as the smaller clusters. Thus, in practice we place one distribution of Sr impurities into the largest (say, $L_3\times L_3$) cluster, and then examine the properties of the $L_1\times L_1$, $L_2\times L_2$, and then $L_3\times L_3$ clusters, etc., to best represent the manner in which the system approaches the bulk limit.

[1] R. J. Birgeneau and G. Shirane, in *Physical Properties of High Temperature Superconductors*, edited by D. M. Ginsberg (World Scientific, Singapore, 1989) Vol. 1, p. 151.
[2] D. C. Johnston, in *Handbook of Magnetic Materials*, edited by K. H. J. Buschow (Elsevier, Amsterdam, 1997).
[3] D. R. Harshmann *et al.*, Phys. Rev. B **38**, 852 (1988); J. I. Budnick *et al.*, Europhys. Lett. **5**, 651 (1988).
[4] S. M. Hayden *et al.*, Phys. Rev. Lett. **66**, 821 (1991).
[5] J. H. Cho *et al.*, Phys. Rev. B **46**, 3179 (1992).
[6] F. C. Chou *et al.*, Phys. Rev. Lett. **75**, 2204 (1995).
[7] B. Keimer *et al.*, Phys. Rev. B **46**, 14 034 (1992).
[8] N. W. Preyer *et al.*, Phys. Rev. B **44**, 407 (1991).
[9] R. J. Gooding, Phys. Rev. Lett. **66**, 2266 (1991).
[10] R. J. Gooding and A. Mailhot, Phys. Rev. B **48**, 6132 (1993).

[11] R. J. Gooding, N. M. Salem, and A. Mailhot, Phys. Rev. B **49**, 6067 (1994).
[12] F. C. Chou *et al.*, Phys. Rev. Lett. **71**, 2323 (1993).
[13] C. Y. Chen *et al.*, Phys. Rev. Lett. **63**, 2307 (1989).
[14] E. Lai and R. J. Gooding (unpublished).
[15] S. Kivelson and V. J. Emery, Physica C **209**, 597 (1991); S. Kivelson and V. J. Emery (unpublished).
[16] K. Yamada *et al.* (unpublished).
[17] B. I. Shraiman and E. D. Siggia, Phys. Rev. Lett. **62**, 1564 (1989).
[18] R. J. Gooding, N. M. Salem, R. J. Birgeneau, and F. C. Chou (unpublished)..
[19] M. Greven *et al.*, Phys. Rev. Lett. **72**, 1096 (1994).
[20] K. J. von Szczepanski, T. M. Rice, and F. C. Zhang, Europhys. Lett. **8**, 797 (1989).
[21] K. M. Rabe and R. Bhatt, J. Appl. Phys. **69**, 4508 (1991).
[22] B. I. Shraiman and E. D. Siggia, Phys. Rev. B **42**, 2485 (1990).
[23] A. A. Belavin and P. M. Polyakov, JETP Lett. **22**, 245 (1975).
[24] One may also derive this result analytically from a perturbed classical nonlinear σ model; K. Beach and R. J. Gooding (unpublished).
[25] P. Gawiec and D. R. Grempel, Phys. Rev. B **44**, 2613 (1993).
[26] J. Vannimenus *et al.*, Phys. Rev. B **39**, 4634 (1989).
[27] F. C. Chou (unpublished).
[28] I. Tanaka, K. Yamane, and H. Kojima, J. Cryst. Growth **96**, 711 (1989).
[29] For example, this gap is equal to $0.28J$ for a 32-site square lattice, J ($\approx$ 1500 K for LaSrCuO) being the AFM exchange constant.
[30] H. Neuberger and T. Ziman, Phys. Rev. B **39**, 2608 (1989).
[31] G. Shirane *et al.*, Phys. Rev. Lett. **63**, 330 (1989).
[32] S.-W. Cheong *et al.*, Phys. Rev. Lett. **67**, 1791 (1991).
[33] T. E. Mason *et al.*, Phys. Rev. Lett. **68**, 1414 (1992); **71**, 919 (1993).
[34] M. Matsuda *et al.*, Phys. Rev. B **49**, 6958 (1994).
[35] J. Villain, J. Phys. C **10**, 4793 (1977); Z. Phys. B **33**, 31 (1979).
[36] J. Budnick (private communication).
[37] Y. Endoh *et al.*, Phys. Rev. B **37**, 7443 (1988).
[38] J. L. Sarrao *et al.* (unpublished).
[39] S. Haas *et al.*, Phys. Rev. Lett. **77**, 3021 (1996).
[40] S. M. Hayden *et al.*, Phys. Rev. Lett. **76**, 1344 (1996).